Published in final edited form as:

*Immunohorizons*. 2018 August ; 2(7): 251–261. doi:10.4049/immunohorizons.1800046.

# The Transcription Factor Runx2 Is Required for Long-Term Persistence of Antiviral CD8+ Memory T Cells

**Elizabeth Olesin**, **Ribhu Nayar**, **Priya Saikumar-Lakshmi**, and **Leslie J. Berg**

Department of Pathology, University of Massachusetts Medical School, Worcester, MA 01605

## Abstract

During acute lymphocytic choriomeningitis virus infection, pathogen-specific $CD8^+$ cytotoxic T lymphocytes undergo clonal expansion leading to viral clearance. Following this, the majority of pathogen-specific $CD8^+$ T cells undergo apoptosis, leaving a small number of memory $CD8^+$ T cells that persist long-term and provide rapid protection upon secondary infection. Whereas much is known about the cytokines and transcription factors that regulate the early effector phase of the antiviral $CD8^+$ T cell response, the factors regulating memory T cell homeostasis and survival are not well understood. In this article, we show that the Runt-related transcription factor Runx2 is important for long-term memory $CD8^+$ T cell persistence following acute lymphocytic choriomeningitis virus-Armstrong infection in mice. Loss of Runx2 in T cells led to a reduction in $KLRG1^{lo}$ $CD127^{hi}$ memory precursor cell numbers with no effect on $KLRG1^{hi}$ $CD127^{lo}$ terminal effector cell populations. Runx2 expression levels were transcriptionally regulated by TCR signal strength via IRF4, TLR4/7, and selected cytokines. These data demonstrate a $CD8^+$ T cell–intrinsic role for Runx2 in the long-term maintenance of antiviral memory $CD8^+$ T cell populations.

## INTRODUCTION

The T cell response to acute viral infections has been well characterized at the cellular level. Following infection, a robust pathogen-specific $CD8^+$ T cell response is observed and within 1–2 wk postinfection, the pathogen is cleared from the infected host. This early effector phase includes the proliferation and differentiation of cytotoxic effector T cells, a process that is dependent on inflammatory cytokines produced by innate immune cells and on the presentation of viral peptides on host APCs (1–3). After viral clearance, the majority of the effector $CD8^+$ T cell population will undergo apoptosis, a process that continues for many weeks post–pathogen clearance (4). Ultimately, the host retains a small pool of pathogen-specific memory T cells that provide rapid protection upon secondary infection (5).



**Address correspondence and reprint requests to:** Dr. Leslie J. Berg, Department of Pathology, University of Massachusetts Medical School, Albert Sherman Center, AS9.1049, 368 Plantation Street, Worcester, MA 01655. Leslie.Berg@umassmed.edu.

The online version of this article contains supplemental material.

DISCLOSURES

The authors have no financial conflicts of interest.

During an acute antiviral response, the pool of activated $CD8^+$ T cells is not homogeneous. Based on differential expression of surface markers, such as KLRG1 and CD127, virus-specific $CD8^+$ T cells can be classified as $KLRG1^{hi}$ $CD127^{lo}$ terminal effector cells (TECs) and $KLRG1^{lo}$ $CD127^{hi}$ memory precursor cells (MPCs) (6). TECs rapidly proliferate in response to infection, make up the majority of the $CD8^+$ effector response, and undergo apoptosis after clearance of the infection. MPCs proliferate less than TECs but go on to survive and undergo homeostatic proliferation alter the infection is eliminated (6, 7). Several transcription factors have been shown to play critical roles in the relative differentiation of TECs versus MPCs during acute viral infection. These include IRF4 (8–12), BATF (13–15), T-bet (16–19), Blimp-1 (20–22), and Id2 (23–26), which regulate TEC differentiation and effector cell function. In contrast, Eomesodermin (Eomes) (17, 19, 27), Tcf1 (28, 29), Id3 (24, 30), and Runx3 (31) are all required for $CD8^+$ T cell memory formation and homeostasis.

In this study, we show that a member of the Runt-related transcription factor family (RUNX), Runx2, is also important for regulating the long-term persistence of $CD8^+$ memory T cells following acute lymphocytic choriomeningitis virus (LCMV)–Armstrong infection. Runx2, like the other RUNX factors, contains a Runt DNA binding domain and pairs with CBFβ to bind to DNA (32). Runx2 functions primarily in bone development in which it is required for osteoblast generation (33) and bone formation (34).

Runx1 and Runx3 have well-characterized roles in T cells, including important functions during regulatory T cell development (35), $T_H1$ skewing (36), and $CD8^+$ T cell differentiation (31, 37). In contrast, no clear function for Runx2 in T cells has been identified, although an earlier study showed that ectopic overexpression of Runx2 in thymocytes perturbed T cell development at the $CD4^-CD8^-$ stage (38). A genome-wide regulatory network generated by Hu and Chen (39) also suggested that Runx2 may play a role in $CD8^+$ T cell memory. Using mice carrying floxed alleles of *Runx2* crossed to CD4-cre, we find no apparent defects in T cell development or T cell homeostasis under steady-state conditions. However, following infection with LCMV–Armstrong, we identify a $CD8^+$ T cell–intrinsic defect in the development and persistence of virus-specific MPCs. This correlates with our findings that Runx2 expression levels in activated $CD8^+$ T cells are enhanced by TLR and memory cytokine stimulation but inhibited by IRF4 expression. Together, these data identify Runx2 as an important mediator of virus-specific memory T cells following resolution of infection by LCMV–Armstrong.

## MATERIALS AND METHODS

### Mice

Mice were bred and housed in specific pathogen-free conditions at the University of Massachusetts Medical School (UMMS) in accordance with Institutional Animal Care and Use Committee guidelines. C57BL/6J mice were purchased from The Jackson Laboratory (Bar Harbor, ME) and bred in house. OT-I TCR transgenic $Rag2^{-/-}$ mice were purchased from Taconic Biosciences (Germantown, NY) and bred in house. $Runx2^{fl/fl}$ mice were a gift from Dr. A. Javed (40) (University of Alabama at Birmingham). $CD4\text{-}cre^+$ transgenic mice were a gift from Dr. J. Kang (UMMS). P14 TCR transgenic mice were a gift from S. Kaech

(Yale University) and were crossed to *Runx2*$^{fl/fl}$ *CD4-cre*$^{+}$ transgenic mice. *Runx2*$^{+/+}$ and *Runx2*$^{+/+}$ *CD4-cre*$^{+}$ mice were used as wild-type (WT) controls. *Irf4*$^{+/fl}$ *CD4-cre*$^{+}$ and *Irf4*$^{fl/fl}$ *CD4-cre*$^{+}$ mice have been described previously (8, 12, 41).

## Virus and infections

Adult male mice (7–11 wk) were infected with LCMV–Armstrong at $5 \times 10^4$ PFU i.p. For rechallenge, mice were infected with LCMV–clone 13 at $2 \times 10^6$ PFU i.v. LCMV–Armstrong and LCMV–clone 13 were graciously provided by Dr. R. Welsh (UMMS). For coadoptive transfers, splenocytes from P14 WT CD4-cre$^{+}$ CD90.1$^{+}$ CD90.2$^{+}$ and P14 *Runx2*$^{fl/fl}$ CD4-cre$^{+}$ CD90.1$^{+}$ were stained with Abs to CD8$\alpha$ and V$\alpha$2 to determine proportions of P14 cells, and equal numbers of WT and *Runx2*$^{fl/fl}$ cells were mixed. Ten thousand P14 cells were transferred i.v. into CD90.2$^{+}$ host mice 1 d prior to infection.

## Plaque assay

Spleens and fat pads were harvested 9 d after LCMV–Armstrong infection. For rechallenge, kidneys and livers were harvested 4 d after LCMV–clone 13 infection. Organs were homogenized in 1 ml RPMI 1640 medium and stored at −80°C. Plaque assays were performed as described previously (42).

## Cell culture

Splenocytes from OT-ITCR transgenic mice were stimulated with OVA, T4, or G4 peptide with indicated doses for 72 h. Cells were harvested and analyzed for Runx2, Eomes, and CD44 expression by intracellular staining. For cytokine experiments, IFN-β and IL-12 were purchased from R&D Systems (Minneapolis, MN). IL-7 and IL-15 were purchased from PeproTech (Rocky Hill, NJ). OVA, T4, and G4 peptides were purchased from 21st Century Biochemicals (Marlborough, MA). Imiquimod was purchased from InvivoGen (San Diego, CA). LPS was purchased from Sigma-Aldrich (St. Louis, MO). Splenocytes from *Irf4*$^{+/+}$ CD4-cre$^{+}$, *Irf4*$^{+/fl}$ CD4-cre$^{+}$,and *Irf4*$^{fl/fl}$ CD4-cre$^{+}$ mice were isolated and plated with plate-bound anti-CD3/CD28 for 72 h. Cells were harvested and analyzed for Runx2, Eomes, and CD44 expression by intracellular staining. For cytokine production, splenocytes from infected mice were stimulated with $gp_{33–41}$, $gp_{276–286}$, and nucleoprotein $(np)_{396–404}$ peptide for 4 h in the presence of 1 μg/ml GolgiStop and 1 μg/ml GolgiPlug and Abs to CD107a and CD107b. $gp_{33–41}$, $gp_{276–286}$, and $np_{396–404}$ peptides were generously provided by Dr. R. Welsh (UMMS) and generated by K. Daniels.

## Ab and H2-D$^{b}$ tetramer staining

CD127 (FITC), Bcl2 (PE), Bcl6 (PE), IRF4 (PE), CD8$\alpha$ (PE–eFluor 610), TNF-$\alpha$ (PerCP–eFluor 710), Eomes (PerCP–eFluor 710), CD122 (PerCP–eFluor 710), T-bet (PE-Cy7), CD44 (PE-Cy7 and Alexa Fluor 700), KLRG1 (PE-Cy7 and eFluor 450), IFN-$\gamma$ (eFluor 450), IL-2 (allophycocyanin), V$\alpha$2 (allophycocyanin), CD27 (allophycocyanin–eFluor 780), and CD90.2 (allophycocyanin–eFluor 780) Abs were purchased from eBioscience (San Diego, CA). CD107a (FITC), CD107b (FITC), CD62L (FITC), 7-AAD, annexin V (PE), and CD90.1 (V500) were purchased from BD Biosciences (Billerica, MA). Abs to granzyme B (PE), LIVE/DEAD Violet, LIVE/DEAD Aqua, and goat anti-rabbit (Alexa Fluor 647)

were purchased from Life Technologies (Grand Island, NY). H2-$D^b$ $gp_{33–41}$, H2-$D^b$ $gp_{276–286}$ and H2-$D^b$ $np_{396–404}$ monomers were obtained from the National Institutes of Health Tetramer Core Facility (Atlanta, GA). Runx2 and TCF-1 Abs were purchased from Cell Signaling Technology (Danvers, MA). Single-cell suspensions from spleens, bone marrow, lymph nodes, lung, and liver were prepared; RBCs were lysed; and Fc receptors were blocked using supernatant from 2.4G2 hybridomas. Lymphocytes were isolated from lung and liver using Lympholyte-M (Cedarlane Laboratories, Burlington, NC), and perfusion was performed on mice to prevent contamination of blood lymphocytes in these preparations. Cells were stained with H2-$D^b$ $gp_{33–41}$, H2-$D^b$ $gp_{276–286}$, and H2-$D^b$ $np_{396–404}$ tetramers prior to staining with cell surface Abs. For cytokine staining, cells were stimulated ex vivo with 1 μg/ml $gp_{33–41}$, $gp_{276–286}$, or $np_{396–404}$ for 4 h at 37°C. Intracellular cytokine staining was performed using BD Cytofix/Cytoperm Fixation/Permeabilization Solution Kit. Intracellular transcription factor staining was performed using eBioscience Foxp3/ Transcription Factor Staining Buffer Set. Samples were analyzed on the LSR II flow cytometer (BD Bioscience), and data were analyzed on Flow Jo (Tree Star).

### Statistical analysis

All data are represented as mean ± SEM. Statistical significance is indicated by $*p \leq 0.05$, $**p \leq 0.01$, $***p \leq 0.001$, and $****p \leq 0.0001$ (NS, $p > 0.05$) based on unpaired Student *t* test.

## RESULTS

### Loss of Runx2 in T cells leads to a defect in pathogen-specific $CD8^+$ MPCs during LCMV–Armstrong infection

To circumvent the neonatal lethality of a germline deficiency in Runx2, we generated mice that lacked Runx2 only in T cells. To this end, $Runx2^{fl/fl}$ mice (40) were crossed to the CD4-$cre^+$ transgenic line (8, 12) (hereafter referred to as $Runx2^{fl/fl}$ mice). $Runx2^{fl/fl}$ mice showed no apparent defect in thymic T cell development or in peripheral T cells compared with $Ranx2^{+/+}$ CD4-$cre^+$ controls (hereafter called WT mice) (Supplemental Fig. 1A–C). Additionally, $Runx2^{fl/fl}$ mice exhibited no abnormalities in their numbers or proportions of $CD8^+CD44^{hi}$ and $CD8^+CD44^{lo}$ T cells within the spleen (Supplemental Fig. 1D).

To assess the function of Runx2 in antiviral T cell responses, we infected WT and $Ranx2^{fl/fl}$ mice with $5 \times 10^4$ PFU LCMV–Armstrong i.p. and harvested spleens at day 9 (the peak of the $CD8^+$ T cell response), day 14 (the attrition phase), and day 28 (the memory phase) postinfection (Fig. 1). Compared with WT mice, $Runx2^{fl/fl}$ mice had no alterations in the numbers of H2-$D^b$ $gp_{33–41}$ tetramer-specific cells (GP33) at days 9 and 14 postinfection but did show reduced numbers of virus-specific cells at day 28 postinfection (Fig. 1A, 1B). Similar results were observed for H2-$D^b$ $gp_{276–286}$–specific cells (GP276) and H2-$D^b$ $np_{396–404}$–specific cells (NP396), indicating the defect at day 28 postinfection in the $CD8^+$ T cells was not an epitope-specific phenotype (Supplemental Fig. 1E).

These results suggested a potential defect in the virus-specific MPC population in LCMV–Armstrong-infected $Ranx2^{fl/fl}$ mice. To assess this possibility, we examined tetramer-

positive CD8$^+$ T cells for KLRG1 and CD127 expression at each time point postinfection. This analysis revealed a defect in the total number of GP33, GP276, and NP396 MPCs in *Runx2$^{fl/fl}$* mice compared with controls at all three time points tested; in contrast, no differences were found in the virus-specific TEC populations in this comparison (Fig. 1C–E, Supplemental Fig. 1F, 1G). Functional memory cells are able to produce IFN-$\gamma$, TNF-$\alpha$, and IL-2, and this polyfunctionality is an indicator of a robust memory population (43). Comparisons of cytokine production by virus-specific WT and *Ranx2$^{fl/fl}$* CD8$^+$ T cells revealed a significant reduction in the total numbers of triple cytokine–producing cells when T cells lacked Runx2 expression (Fig. 1F, Supplemental Fig. 1K). These data indicated that the reduced numbers of tetramer-positive CD8$^+$ T cells in LCMV–Armstrong-infected *Runx2$^{fl/fl}$* mice was due to a defect in the memory T cell population.

As mentioned above, *Ranx2$^{fl/fl}$* mice showed no reduction in virus-specific TEC numbers compared with WT mice at days 9, 14, or 28 after LCMV infection. We also observed only modest defects in granzyme B expression and no defects in CD107a+b expression at day 9 postinfection in *Runx2$^{fl/fl}$* mice (Supplemental Fig. 1H, 1I). These results suggested there were no defects in antiviral effector cell functions when T cells lacked Runx2. Analysis of viral clearance in LCMV–Armstrong-infected WT versus *Runx2$^{fl/fl}$* mice confirmed this supposition (Supplemental Fig. 1J).

Based on these data, we considered whether virus-specific CD8$^+$ T cell subsets might express different levels of Runx2. To test this, we infected WT C57/BL6 mice with LCMV–Armstrong and harvested spleens at day 9 postinfection. Runx2 protein levels were examined in CD8$^+$ MPCs and TECs specific for three viral epitopes. Although Runx2 was upregulated in both subsets of virus-specific cells relative to the levels present in naive CD8$^+$ T cells, we observed increased levels of Runx2 in the MPCs compared with the TECs for each of the epitopes tested (Fig. 1G). These results indicated that Runx2 is upregulated within all activated CD8$^+$ T cells but is higher within the MPC population than in the TEC subset.

To further assess potential molecular differences between WT and *Runx2$^{fl/fl}$* antiviral CD8$^+$ T cells, we examined the expression levels of several transcription factors that are important for TEC and MPC differentiation and function. This analysis revealed that at days 14 and 28 postinfection, *Ranx2$^{fl/fl}$* CD8$^+$ T cells expressed lower levels of Eomes and TCF-1 compared with WT T cells, consistent with the reduced number of MPCs in these mice. In contrast, expression of T-bet, a factor associated with CD8$^+$ effector function, was not altered between WT and *Runx2$^{fl/fl}$* cells (Fig. 1H, Supplemental Fig. 1L, 1M), consistent with previous results indicating no defect in CD8$^+$ effector function (Supplemental Fig. 1H, 1I).

We next considered whether the loss of MPCs in LCMV–Armstrong-infected *Runx2$^{fl/fl}$* mice were due to Runx2 promoting apoptosis in MPCs. However, examination of splenocytes from LCMV–Armstrong-infected WT or *Ranx2$^{fl/fl}$* mice at day 10 postinfection failed to show a significant increase in apoptosis of virus-specific CD8$^+$ T cells in the absence of Runx2 (Supplemental Fig. 2). Taken together, these results indicated that Runx2 is regulating an alternative aspect of memory CD8$^+$ T cell persistence, such as homeostatic proliferation, rather than survival.

## Loss of pathogen-specific CD8+ memory T cells is due to a CD8+ T cell–intrinsic deficiency in Runx2

To determine whether the loss of LCMV-specific Runx2-deficient $CD8^+$ memory T cells was caused by an intrinsic loss of Runx2 in the $CD8^+$ T cells, we performed adoptive transfer experiments. WT and *Runx2*$^{fl/fl}$ mice were crossed to the P14 TCR transgenic line that expresses a TCR specific for the GP33 epitope of LCMV. WT ($CD90.1^+$ $CD90.2^+$) and *Runx2*$^{fl/fl}$ ($CD90.1^+$) P14 cells were cotransferred into $CD90.2^+$ host mice at a 1:1 mixture (Fig. 2A), and recipients were infected with LCMV–Armstrong the following day. Four weeks later, donor cells were examined in the spleens of infected mice. As shown in Fig. 2, *Runx2*$^{fl/fl}$ P14 cells were significantly reduced in numbers relative to WT P14 cells (Fig. 2B). Assessment of TEC and MPC subsets showed that both populations of *Runx2*$^{fl/fl}$ P14 cells were reduced in numbers compared with their WT counterparts, but a more dramatic reduction was observed in the *Runx2*$^{fl//fl}$ MPC subset, in which WT P14 cells outnumbered *Runx2*$^{fl/fl}$ P14 cells by a 23-fold margin (Fig. 2C). Examination of several proteins associated with MPC differentiation and survival, including Eomes, TCF-1, CD27, CD122, and Bcl2, showed reduced expression by *Runx2*$^{fl/fl}$ P14 cells relative to WT P14 cells at this time point. Surprisingly, this was not the case for Bcl6, which was upregulated in *Runx2*$^{fl/fl}$ cells compared with WT controls (Fig. 2D). We also assessed cytokine production by WT and *Runx2*$^{fl/fl}$ P14 cells at day 28 postinfection and observed markedly fewer triple cytokine-producing cells among the *Runx2*$^{fl/fl}$ P14 cells relative to WT P14 cells (Fig. 2E). Overall, these data demonstrate that the defect in memory $CD8^+$ T cell persistence in *Runx2*$^{fl/fl}$ mice following LCMV–Armstrong infection is a $CD8^+$ T cell–intrinsic phenotype.

## Runx2-dependent CD8+ memory T cell loss does not impair the recall response to LCMV

To determine whether the defect in numbers of *Runx2*$^{fl/fl}$ $CD8^+$ memory T cells would impact the recall response, we rechallenged LCMV–Armstrong-infected WT and *Runx2*$^{fl/fl}$ mice with LCMV–clone 13. Initially, WT and *Runx2*$^{fl/fl}$ mice were infected with LCMV–Armstrong, and 90 d postinfection, mice were rechallenged with a high dose of LCMV–clone 13. Prior to rechallenge, we examined the surviving populations of virus-specific $CD8^+$ T cells and found reduced numbers of tetramer-positive cells in *Runx2*$^{fl/fl}$ mice compared with controls; furthermore, *Runx2*$^{fl/fl}$ mice had a more substantial deficit in the $CD62L^{hi}$ than in the $CD62L^{lo}$ subset of each epitope-specific memory T cell population (Fig. 3A, Supplemental Fig. 3A–C). Four days after rechallenge, we observed substantial expansion of both the WT and *Runx2*$^{fl/fl}$ virus-specific memory cells. This robust recall response was observed for all three viral epitopes tested (Fig. 3B, Supplemental Fig. 3D). A careful examination of TECs and MPCs showed no significant differences in either population when comparing WT to *Runx2*$^{fl/fl}$ mice (Fig. 3C). We also found no differences in viral clearance between WT and *Runx2*$^{fl/fl}$ at day 4 post-rechallenge (Fig. 3D). Phenotypic and functional analysis of the cells after rechallenge showed few significant differences between virus-specific WT and *Runx2*$^{fl/fl}$ cells (Fig. 3E, Supplemental Fig. 3E–J). These results indicate that the loss of memory T cells seen in *Runx2*$^{fl/fl}$ mice does not impair their protective response to secondary challenge.

Based on these data, we considered whether the reduced numbers of virus-specific memory $CD8^+$ T cells seen in the spleens of *Runx2*$^{fl/fl}$ mice might be due to altered migration of

these cells to other tissues rather than to an absolute reduction in the total memory cell population. This hypothesis was suggested by a previous study that showed loss of Runx2 in the plasmacytoid dendritic cell compartment led to a retention of the cells in the bone marrow (44). To test this, we examined several organs for pathogen-specific $CD8^+$ T cells 14 d after primary infection with LCMV–Armstrong. As shown, we found significantly fewer LCMV-specific memory $CD8^+$ T cells in nearly all organs examined and for each of the viral epitopes assessed (Fig. 3F, Supplemental Fig. 3K, 3L). These data indicate that the reduced numbers of splenic *Runx2*$^{fl/fl}$ LCMV-specific memory $CD8^+$ T cells is not due to enhanced homing or retention of these cells to or in other organs.

## Runx2 expression is regulated by TLR4/TLR7 signals and cytokine signaling pathways in vitro

Previous work has shown a role for TLR signaling in $CD8^+$ T cell memory formation (45, 46). We next wanted to determine if Runx2 expression in activated $CD8^+$ T cells was regulated by TLR signaling in vitro. To determine the optimal day poststimulation to look at Runx2 expression, we isolated splenocytes from P14 TCR transgenic mice and looked for Runx2 expression up to 5 d after stimulation with GP33 peptide. We found that Runx2 was up-regulated by day 3 poststimulation and remained elevated through day 5 (Supplemental Fig. 4A); however, cell death increased dramatically starting at day 4 postinfection (Supplemental Fig. 4B). We therefore chose 72 h poststimulation as the optimal time point for assessing Runx2 expression accompanied by minimal cell death in vitro. To test the role of TLR agonists on Runx2 expression, we isolated splenocytes from OT-I TCR transgenic *Rag2*$^{-/-}$ mice, stimulated OT-I T cells with high or low concentrations of the lower-affinity OVA peptide variant SIITFEKL (T4), and incubated with or without TLR agonists LPS (Fig. 4A) or imiquimod (Fig. 4B). We found that Runx2 was upregulated in cells treated with either TLR agonist at both high and low T4 peptide doses, but this upregulation was more dramatic when cells were stimulated with the low peptide dose.

Previous work from M. Mescher and colleagues (47, 48) has shown that type I IFN and IL-12 regulate memory $CD8^+$ T cell development in several viral and intracellular bacterial infection systems. These findings prompted us to assess whether type I IFN or IL-12 was contributing to the high expression of Runx2 in $CD8^+$ T cells stimulated in the presence of TLR agonists. We stimulated OT-I T cells with either a high or low concentration of T4 peptide and incubated cells with or without IFN-β (Fig. 4C) or IL-12 (Fig. 4D). We found treatment with IFN-β had no significant effect on Runx2 expression, whereas treatment with IL-12 led to increased Runx2 expression at the lower peptide dose. These results suggest a direct effect of IL-12 on T cells. Furthermore, the fact that IFN-β had no direct effect on T cells suggests that the enhanced Runx2 upregulation observed when stimulation cultures were treated with TLR agonists might be acting via upregulation of costimulatory molecules on splenic APCs.

We also tested additional cytokines known to be important in homeostatic proliferation and survival of memory cells for their effects on Runx2 expression. Splenocytes from OT-I TCR transgenic mice were isolated and stimulated with high or low doses of the T4 peptide. Cultures were supplemented with or without IL-7 (Fig. 4E) or IL-15 (Fig. 4F) and analyzed

at day 3 poststimulation. These studies demonstrated that both IL-7 and IL-15 promoted increased expression of Runx2 when T cells were activated with weak TCR stimulation.

Together, these data show that TLR signaling, most likely in APCs, and stimulation of T cells with cytokines known to be important in $CD8^+$ T cell memory development and homeostasis enhance Runx2 upregulation; interestingly, these cytokines and TLR agonist signals have the greatest impact in T cells activated with weaker strength of TCR signaling.

### Runx2 expression is regulated by TCR signaling pathways in activated $CD8^+$ T cells in vitro

From our TLR and cytokine data, we found that OT-I cells stimulated with low concentrations of T4 peptide expressed higher levels of Runx2 than cells stimulated with a higher concentration of peptides (Fig. 4). These data suggested an important role for TCR signal strength in controlling Runx2 expression levels. Previous studies have shown an important inverse correlation between TCR signal strength and the development of $CD8^+$ MPCs postinfection (3, 49). To assess more comprehensively a role for TCR signal strength in regulating Runx2 expression, we performed experiments using extensive dose ranges of three peptides recognized by the OT-I TCR. For these studies, OT-I cells were stimulated with APCs plus various concentrations of the highly potent SIINFEKL (OVA) peptide, the medium potency (T4) peptide, or the low potency SIIGFEKL (G4) peptide. These experiments clearly revealed an inverse correlation between peptide dose and Runx2 expression (Fig. 5A). Similar results were also observed for Eomes expression (Fig. 5B). As expected, CD44 upregulation showed a positive correlation with peptide dose (Fig. 5C).

These findings suggested that the transcription factor IRF4 might regulate Runx2 expression. This possibility was suggested by our previous studies showing that IRF4 is upregulated to different levels based on TCR signal strength and, further, that IRF4 is a negative regulator of Eomes expression (8, 12). To test this possibility, we stimulated WT, $Irf4^{+/fl}$ $CD4\text{-}cre^+$, and $Irf4^{fl/fl}$ $CD4\text{-}cre^+$ (hereby referred to as $Irf4^{+/fl}$ and $Irf4^{fl/fl}$, respectively) naive $CD8^+$ T cells with anti-CD3/CD28 for 72 h and examined Runx2 expression. As shown, we observed a significant increase in Runx2 expression in stimulated $Irf4^{fl/fl}$ $CD8^+$ T cells compared with WT or $Irf4^{+/fl}$ cells (Fig. 5D). Consistent with previously published data, similar results were observed for Eomes (Fig. 5E). Together, these results indicate that Runx2 is more highly expressed when $CD8^+$ T cells are stimulated with low levels of Ag and that IRF4 is a negative regulator of Runx2 and Eomes expression following $CD8^+$ T cell activation.

## DISCUSSION

A key aspect of the adaptive immune response is the generation of long-term memory cells that provide rapid and robust protection upon secondary exposure to an infecting pathogen. Improving memory $CD8^+$ T cell responses is currently a focus of many vaccine efforts, whereas inhibition of memory T cell responses is an ongoing challenge in the development of therapies to treat autoimmune diseases. Thus, there is a need to understand in more detail the molecular mechanisms regulating memory T cell development and persistence.

Our studies identified Runx2 as an important factor in the maintenance of long-term memory $CD8^+$ T cells. However, we found that Runx2 was not necessary for antiviral effector function or for robust recall responses to secondary challenge. These features of the $CD8^+$ T cell response to infection in *Runx2*$^{fl/fl}$ mice show a striking resemblance to previous studies examining the consequences of a deficiency in IL-15 or IL-15Ra (50–52). In these earlier studies, IL-15 signaling was found to be essential for long-term memory $CD8^+$ T cell homeostasis and self-renewal. We observed that IL-15 stimulation of $CD8^+$ T cells in vitro promoted enhanced Runx2 upregulation only under conditions of weak TCR stimulation. These findings suggest the possibility that in vivo tonic TCR signals plus IL-15 are functioning to maintain memory cells in part through the upregulation of Runx2. Consistent with this possibility, IL-15 is thought to promote memory T cell homeostatic proliferation rather than memory cell survival (53–57), a function that aligns well with data demonstrating that Runx2 overexpression in thymocytes promotes uncontrolled cellular proliferation leading to lymphomagenesis (58).

We also found that Runx2 expression levels are enhanced by weak rather than strong TCR signal intensity, likely because of negative regulation by the transcription factor IRF4. This pattern mirrors that of Eomes, another transcription factor associated with long-term memory $CD8^+$ T cell maintenance (27). Along with weak TCR signaling, cytokines that promote memory T cell formation and signals that activate APCs also promote enhanced Runx2 upregulation. These data further strengthen an association of Runx2 expression with optimal formation of long-lived memory $CD8^+$ T cells (5, 49).

Determining the precise mechanism underlying the loss of memory $CD8^+$ T cells in the absence of Runx2 has remained. Early on, studies using microarrays were performed to identify differentially expressed genes between WT and *Runx2*$^{fl/fl}$ $CD8^+$ T cells. Cells isolated from LCMV–Armstrong-infected mice and analyzed directly ex vivo failed to yield informative gene targets of Runx2 regulation; similar uninformative results were obtained when comparing WT and *Runx2*$^{fl/fl}$ $CD8^+$ T cells stimulated in vitro (data not shown). This prompted us to consider alternative mechanisms for Runx2 function, such as a change in rRNA transcription and processing, based on the known role for Runx2 in regulating this pathway in osteoblasts (59); these studies also failed to identify a function for Runx2 in $CD8^+$ T cells (data not shown). One additional possibility is that Runx2 is affecting memory formation through regulation of chromatin accessibility, a known function of Runx3 in $CD8^+$ T cells (31). RUNX family members have been shown to have redundant roles in $CD4^+$ regulatory T cells; thus, the most robust alterations are observed in the absence of Cbfβ, the binding partner for all three Runx proteins (60). Future studies examining $CD8^+$ T cell memory using Cbfβ-deficient T cells may be informative in this regard. Alternatively, Runx2 may function intermittently in memory $CD8^+$ T cells during short time windows when memory cells associate with stromal cells in lymphoid organs and receive homeostatic TCR and IL-15/IL-7 signals. Capturing the cells during these brief interactions may be required to identify the specific genes and/or pathways regulated by Runx2 in memory $CD8^+$ T cells.

## Supplementary Material

Refer to Web version on PubMed Central for supplementary material.

## ACKNOWLEDGMENTS

We thank Dr. Raymond Welsh and Dr. Lucio Castilla for insightful discussions. We thank Dr. Amjad Javed for the *Runx*$^{fl/fl}$ mouse line, Regina Whitehead and Sharlene Hubbard for technical assistance, and the National Institutes of Health Tetramer Core Facility for LCMV-specific H2-D$^{b}$ $gp_{33–41}$, $gp_{276–286}$, and $np_{396–404}$ monomers.

This work was supported by the National Institutes of Health (AI132419).

## Abbreviations used in this article:

| | |
|---|---|
| **Eomes** | Eomesodermin |
| **GP33** | H2-D$^{b}$ $gp_{33–41}$ tetramer–specific cell |
| **LCMV** | lymphocytic choriomeningitis virus |
| **MPC** | memory precursor cell |
| **np** | nucleoprotein |
| **TEC** | terminal effector cell |
| **UMMS** | University of Massachusetts Medical School |
| **WT** | wild-type |

## REFERENCES

1. Mempel TR, Henrickson SE, and Von Andrian UH. 2004 T-cell priming by dendritic cells in lymph nodes occurs in three distinct phases. Nature 427: 154–159. [PubMed: 14712275]
2. Wherry EJ, and Ahmed R. 2004 Memory CD8 T-cell differentiation during viral infection. J. Virol. 78: 5535–5545. [PubMed: 15140950]
3. Kaech SM, and Cui W. 2012 Transcriptional control of effector and memory CD8$^{+}$ T cell differentiation. Nat. Rev. Immunol. 12: 749–761. [PubMed: 23080391]
4. Zhou X, Ramachandran S, Mann M, and Popkin DL. 2012 Role of lymphocytic choriomeningitis virus (LCMV) in understanding viral immunology: past, present and future. Viruses 4: 2650–2669. [PubMed: 23202498]
5. Cui W, and Kaech SM. 2010 Generation of effector CD8$^{+}$ T cells and their conversion to memory T cells. Immunol. Rev. 236: 151–166. [PubMed: 20636815]
6. Kaech SM, Tan JT, Wherry EJ, Konieczny BT, Surh CD, and Ahmed R. 2003 Selective expression of the interleukin 7 receptor identifies effector CD8 T cells that give rise to long-lived memory cells. Nat. Immunol. 4: 1191–1198. [PubMed: 14625547]
7. Joshi NS, and Kaech SM. 2008 Effector CD8 T cell development: a balancing act between memory cell potential and terminal differentiation. J. Immunol. 180: 1309–1315. [PubMed: 18209024]
8. Nayar R, Enos M, Prince A, Shin H, Hemmers S, Jiang J-K, Klein U, Thomas CJ, and Berg LJ. 2012 TCR signaling via Tec kinase ITK and interferon regulatory factor 4 (IRF4) regulates CD8$^{+}$ T-cell differentiation. Proc. Natl. Acad. Sci. USA 109: E2794–E2802. [PubMed: 23011795]
9. Raczkowski F, Ritter J, Heesch K, Schumacher V, Guralnik A, ocker LH, Raifer H, Klein M, Bopp T, Harb H, et al. 2013 The transcription factor interferon regulatory factor 4 is required for the generation of protective effector CD8$^{+}$ T cells. Proc. Natl. Acad. Sci. USA 110: 15019–15024. [PubMed: 23980171]

10. Man K, Miasari M, Shi W, Xin A, Henstridge DC, Preston S, Pellegrini M, Belz GT, Smyth GK, Febbraio MA, et al. 2013 The transcription factor IRF4 is essential for TCR affinity-mediated metabolic programming and clonal expansion of T cells. Nat. Immunol. 14: 1155–1165. [PubMed: 24056747]
11. Yao S, Buzo BF, Pham D, Jiang L, Taparowsky EJ, Kaplan MH, and Sun J. 2013 Interferon regulatory factor 4 sustains CD8(+) T cell expansion and effector differentiation. Immunity 39: 833–845. [PubMed: 24211184]
12. Nayar R, Schutten E, Bautista B, Daniels K, Prince AL, Enos M, Brehm MA, Swain SL, Welsh RM, and Berg LJ. 2014 Graded levels of IRF4 regulate CD8+ T cell differentiation and expansion, but not attrition, in response to acute virus infection. J. Immunol. 192: 5881–5893. [PubMed: 24835398]
13. Kurachi M, Barnitz RA, Yosef N, Odorizzi PM, DiIorio MA, Lemieux ME, Yates K, Godec J, Klatt MG, Regev A, et al. 2014 The transcription factor BATF operates as an essential differentiation checkpoint in early effector CD8+ T cells. Nat. Immunol. 15: 373–383. [PubMed: 24584090]
14. Grusdat M, McIlwain DR, Xu HC, Pozdeev VI, Knievel J, Crome SQ, Robert-Tissot C, Dress RJ, Pandyra AA, Speiser DE, et al. 2014 IRF4 and BATF are critical for CD8+ T-cell function following infection with LCMV. Cell Death Differ. 21: 1050–1060. [PubMed: 24531538]
15. Godec J, Cowley GS, Barnitz RA, Alkan O, Root DE, Sharpe AH, and Haining WN. 2015 Inducible RNAi in vivo reveals that the transcription factor BATF is required to initiate but not maintain CD8+ T-cell effector differentiation. [Published erratum appears in 2015 Proc. Natl. Acad. Sci. USA 112: E4968.] Proc. Natl. Acad. Sci. USA 112: 512–517. [PubMed: 25548173]
16. Sullivan BM, Juedes A, Szabo SJ, von Herrath M, and Glimcher LH. 2003 Antigen-driven effector CD8 T cell function regulated by T-bet. Proc. Natl. Acad. Sci. USA 100: 15818–15823. [PubMed: 14673093]
17. Intlekofer AM, Takemoto N, Wherry EJ, Longworth SA, Northrup JT, Palanivel VR, Mullen AC, Gasink CR, Kaech SM, Miller JD, et al. 2005 Effector and memory CD8+ T cell fate coupled by T-bet and Eomesodermin. [Published erratum appears in 2006 Nat. Immunol. 7: 113.] Nat. Immunol 6: 1236–1244. [PubMed: 16273099]
18. Joshi NS, Cui W, Chandele A, Lee HK, Urso DR, Hagman J, Gapin L, and Kaech SM. 2007 Inflammation directs memory precursor and short-lived effector CD8(+) T cell fates via the graded expression of T-bet transcription factor. Immunity 27: 281–295. [PubMed: 17723218]
19. Rao RR, Li Q, Odunsi K, and Shrikant PA. 2010 The mTOR kinase determines effector versus memory CD8+ T cell fate by regulating the expression of transcription factors T-bet and Eomesodermin. Immunity 32: 67–78. [PubMed: 20060330]
20. Rutishauser RL, Martins GA, Kalachikov S, Chandele A, Parish IA, Meffre E, Jacob J, Calame K, and Kaech SM. 2009 Transcriptional repressor Blimp-1 promotes CD8(+) T cell terminal differentiation and represses the acquisition of central memory T cell properties. Immunity 31: 296–308. [PubMed: 19664941]
21. Shin HM, Kapoor V, Guan T, Kaech SM, Welsh RM, and Berg LJ. 2013 Epigenetic modifications induced by Blimp-1 Regulate CD8+ T cell memory progression during acute virus infection. Immunity 39: 661–675. [PubMed: 24120360]
22. Xin A, Masson F, Liao Y, Preston S, Guan T, Gloury R, Olshansky M, Lin J-X, Li P, Speed TP, et al. 2016 A molecular threshold for effector CD8(+) T cell differentiation controlled by transcription factors Blimp-1 and T-bet. Nat. Immunol. 17: 422–432.
23. Cannarile MA, Lind NA, Rivera R, Sheridan AD, Camfield KA, Wu BB, Cheung KP, Ding Z, and Goldrath AW. 2006 Transcriptional regulator Id2 mediates CD8+ T cell immunity. Nat. Immunol. 7: 1317–1325. [PubMed: 17086188]
24. Yang CY, Best JA, Knell J, Yang E, Sheridan AD, Jesionek AK, Li HS, Rivera RR, Lind KC, D'Cruz LM, et al. 2011 The transcriptional regulators Id2 and Id3 control the formation of distinct memory CD8+ T cell subsets. Nat. Immunol. 12: 1221–1229. [PubMed: 22057289]
25. Knell J, Best JA, Lind NA, Yang E, D'Cruz LM, and Goldrath AW. 2013 Id2 influences differentiation of killer cell lectinlike receptor G1(hi) short-lived CD8+ effector T cells. J. Immunol. 190:1501–1509. [PubMed: 23325888]

26. Omilusik KD, Nadjsombati MS, Shaw LA, Yu B, Milner JJ, and Goldrath AW. 2018 Sustained Id2 regulation of E proteins is required for terminal differentiation of effector $CD8^+$ T cells. J. Exp. Med. 215: 773–783. [PubMed: 29440362]
27. Banerjee A, Gordon SM, Intlekofer AM, Paley MA, Mooney EC, Lindsten T, Wherry EJ, and Reiner SL. 2010 Cutting edge: the transcription factor Eomesodermin enables $CD8^+$ T cells to compete for the memory cell niche. J. Immunol. 185: 4988–4992. [PubMed: 20935204]
28. Jeannet G, Boudousquié C, Gardiol N, Kang J, Huelsken J, and Held W. 2010 Essential role of the Wnt pathway effector Tcf-1 for the establishment of functional CD8 T cell memory. Proc. Natl. Acad. Sci. USA 107: 9777–9782. [PubMed: 20457902]
29. Zhou X, Yu S, Zhao D-M, Harty JT, Badovinac VP, and Xue H-H. 2010 Differentiation and persistence of memory $CD8(^+)$T cells depend on T cell factor 1. Immunity 33: 229–240. [PubMed: 20727791]
30. Ji Y, Pos Z, Rao M, Klebanoff CA, Yu Z, Sukumar M, Reger RN, Palmer DC, Borman ZA, Muranski P, et al. 2011 Repression of the DNA-binding inhibitor Id3 by Blimp-1 limits the formation of memory $CD8^+$ T cells. Nat. Immunol. 12: 1230–1237. [PubMed: 22057288]
31. Wang D, Diao H, Getzler AJ, Rogal W, Frederick MA, Milner J, Yu B, Crotty S, Goldrath AW, and Pipkin ME. 2018 The transcription factor Runx3 establishes chromatin accessibility of cisregulatory landscapes that drive memory cytotoxic T lymphocyte formation. Immunity 48: 659–674.e6. [PubMed: 29669249]
32. Tahirov TH, Inoue-Bungo T, Morii H, Fujikawa A, Sasaki M, Kimura K, Shiina M, Sato K, Kumasaka T, Yamamoto M, et al. 2001 Structural analyses of DNA recognition by the AML1/Runx-1 Runt domain and its allosteric control by CBFbeta. Cell 104: 755–767. [PubMed: 11257229]
33. Komori T 2018 Runx2, an inducer of osteoblast and chondrocyte differentiation. Histochem. Cell Biol. 149: 313–323. [PubMed: 29356961]
34. Choi JY, Pratap J, Javed A, Zaidi SK, Xing L, Balint E, Dalamangas S, Boyce B, van Wijnen AJ, Lian JB, et al. 2001 Subnuclear targeting of Runx/Cbfa/AML factors is essential for tissue-specific differentiation during embryonic development. Proc. Natl. Acad. Sci. USA 98: 8650–8655. [PubMed: 11438701]
35. Kitoh A, Ono M, Naoe Y, Ohkura N, Yamaguchi T, Yaguchi H, Kitabayashi I, Tsukada T, Nomura T, Miyachi Y, et al. 2009 Indispensable role of the Runx1-Cbfbeta transcription complex for in vivo-suppressive function of FoxP3+ regulatory T cells. Immunity 31: 609–620. [PubMed: 19800266]
36. Naoe Y, Setoguchi R, Akiyama K, Muroi S, Kuroda M, Hatam F, Littman DR, and Taniuchi I. 2007 Repression of interleukin-4 in T helper type 1 cells by Runx/Cbf β binding to the *Il4* silencer. J. Exp. Med. 204: 1749–1755. [PubMed: 17646405]
37. Cruz-Guilloty F, Pipkin ME, Djuretic IM, Levanon D, Lotem J, Lichtenheld MG, Groner Y, and Rao A. 2009 Runx3 and T-box proteins cooperate to establish the transcriptional program of effector CTLs. J. Exp. Med. 206: 51–59. [PubMed: 19139168]
38. Vaillant F, Blyth K, Andrew L, Neil JC, and Cameron ER. 2002 Enforced expression of Runx2 perturbs T cell development at a stage coincident with beta-selection. J. Immunol. 169: 2866–2874. [PubMed: 12218099]
39. Hu G, and Chen J. 2013 A genome-wide regulatory network identifies key transcription factors for memory $CD8^+$ T-cell development. Nat. Commun. 4: 2830. [PubMed: 24335726]
40. Chen H, Ghori-Javed FY, Rashid H, Serra R, Gutierrez SE, and Javed A. 2011 Chondrocyte-specific regulatory activity of Runx2 is essential for survival and skeletal development. Cells Tissues Organs 194: 161–165. [PubMed: 21597273]
41. Klein U, Casola S, Cattoretti G, Shen Q, Lia M, Mo T, Ludwig T, Rajewsky K, and Dalla-Favera R. 2006 Transcription factor IRF4 controls plasma cell differentiation and class-switch recombination. Nat. Immunol. 7: 773–782. [PubMed: 16767092]
42. Welsh RM, and Seedhom MO. 2008 Lymphocytic choriomeningitis virus (LCMV): propagation, quantitation, and storage. Curr. Protoc. Microbiol. Chapter 15: Unit 15A.1.
43. Slifka MK, and Whitton JL. 2000 Activated and memory $CD8^+$ T cells can be distinguished by their cytokine profiles and phenotypic markers. J. Immunol. 164: 208–216. [PubMed: 10605013]

44. Chopin M, Preston SP, Lun ATL, Tellier J, Smyth GK, Pellegrini M, Belz GT, Corcoran LM, Visvader JE, Wu L, and Nutt SL. 2016 RUNX2 mediates plasmacytoid dendritic cell egress from the bone marrow and controls viral immunity. Cell Rep. 15: 866–878. [PubMed: 27149837]
45. Quigley M, Martinez J, Huang X, and Yang Y. 2009 A critical role for direct TLR2-MyD88 signaling in CD8 T-cell clonal expansion and memory formation following vaccinia viral infection. Blood 113: 2256–2264. [PubMed: 18948575]
46. Mercier BC, Cottalorda A, Coupet CA, Marvel J, and Bonnefoy-Bérard N. 2009 TLR2 engagement on CD8 T cells enables generation of functional memory cells in response to a suboptimal TCR signal. J. Immunol. 182: 1860–1867. [PubMed: 19201838]
47. Xiao Z, Casey KA, Jameson SC, Curtsinger JM, and Mescher MF. 2009 Programming for CD8 T cell memory development requires IL-12 or type I IFN. J. Immunol. 182: 2786–2794. [PubMed: 19234173]
48. Agarwal P, Raghavan A, Nandiwada SL, Curtsinger JM, Bohjanen PR, Mueller DL, and Mescher MF. 2009 Gene regulation and chromatin remodeling by IL-12 and type I IFN in programming for CD8 T cell effector function and memory. J. Immunol. 183: 1695–1704. [PubMed: 19592655]
49. Restifo NP, and Gattinoni L. 2013 Lineage relationship of effector and memory T cells. Curr. Opin. Immunol. 25: 556–563. [PubMed: 24148236]
50. Lodolce JP, Boone DL, Chai S, Swain RE, Dassopoulos T, Trettin S, and Ma A. 1998 IL-15 receptor maintains lymphoid homeostasis by supporting lymphocyte homing and proliferation. Immunity 9: 669–676. [PubMed: 9846488]
51. Kennedy MK, Glaccum M, Brown SN, Butz EA, Viney JL, Embers M, Matsuki N, Charrier K, Sedger L, Willis CR, et al. 2000 Reversible defects in natural killer and memory CD8 T cell lineages in interleukin 15-deficient mice. J. Exp. Med. 191: 771–780. [PubMed: 10704459]
52. Ma A, Koka R, and Burkett P. 2006 Diverse functions of IL-2, IL-15, and IL-7 in lymphoid homeostasis. Annu. Rev. Immunol. 24: 657–679. [PubMed: 16551262]
53. Becker TC, Wherry EJ, Boone D, Murali-Krishna K, Antia R, Ma A, and Ahmed R. 2002 Interleukin 15 is required for proliferative renewal of virus-specific memory CD8 T cells. J. Exp. Med. 195: 1541–1548. [PubMed: 12070282]
54. Schluns KS, Williams K, Ma A, Zheng XX, and Lefrançois L. 2002 Cutting edge: requirement for IL-15 in the generation of primary and memory antigen-specific CD8 T cells. J. Immunol. 168: 4827–4831. [PubMed: 11994430]
55. Goldrath AW, Sivakumar PV, Glaccum M, Kennedy MK, Bevan MJ, Benoist C, Mathis D, and Butz EA. 2002 Cytokine requirements for acute and basal homeostatic proliferation of naive and memory $CD8^+$ T cells. J. Exp. Med. 195: 1515–1522. [PubMed: 12070279]
56. Burkett PR, Koka R, Chien M, Chai S, Chan F, Ma A, and Boone DL. 2003 IL-15R alpha expression on $CD8^+$ T cells is dispensable for T cell memory. Proc. Natl. Acad. Sci. USA 100: 4724–4729. [PubMed: 12671073]
57. Rubinstein MP, Lind NA, Purton JF, Filippou P, Best JA, McGhee PA, Surh CD, and Goldrath AW. 2008 IL-7 and IL-15 differentially regulate $CD8^+$ T-cell subsets during contraction of the immune response. Blood 112: 3704–3712. [PubMed: 18689546]
58. Vaillant F, Blyth K, Terry A, Bell M, Cameron ER, Neil J, and Stewart M. 1999 A full-length Cbfa1 gene product perturbs T-cell development and promotes lymphomagenesis in synergy with myc. Oncogene 18: 7124–7134. [PubMed: 10597314]
59. Ali SA, Dobson JR, Lian JB, Stein JL, van Wijnen AJ, Zaidi SK, and Stein GS. 2012 A RUNX2-HDAC1 co-repressor complex regulates rRNA gene expression by modulating UBF acetylation. J. Cell Sci. 125: 2732–2739. [PubMed: 22393235]
60. Rudra D, Egawa T, Chong MMW, Treuting P, Littman DR, and Rudensky AY. 2009 Runx-CBFbeta complexes control expression of the transcription factor Foxp3 in regulatory T cells. Nat. Immunol. 10: 1170–1177. [PubMed: 19767756]

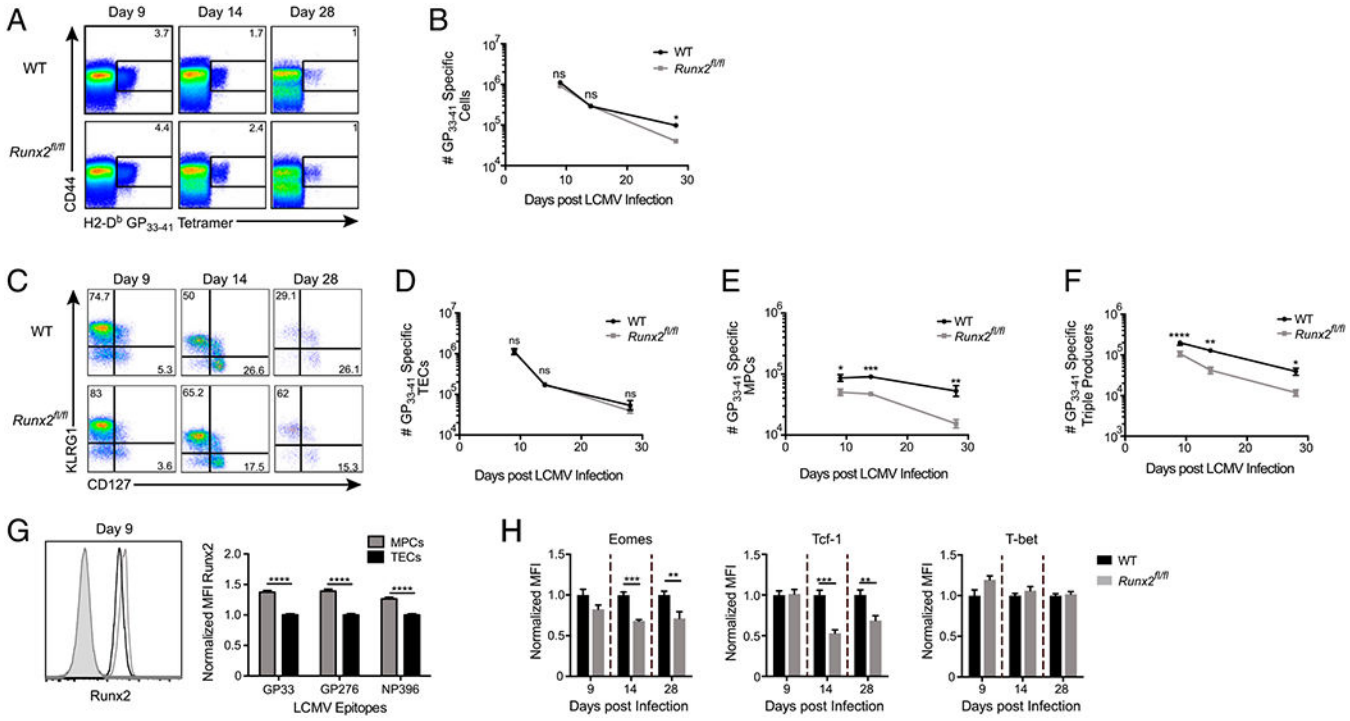


**FIGURE 1. Loss of Runx2 in the T cell compartment leads to a defect in the number of CD8$^+$ memory precursor T cells during LCMV–Armstrong infection.**

WT and *Runx2$^{fl/fl}$* mice were infected with LCMV–Armstrong and analyzed on days 9, 14, and 28 postinfection. (**A**) Gated CD8$\alpha^+$ splenocytes were stained for H2-D$^b$ gp$_{33–41}$ tetramer and CD44. (**B**) Compilation of data shows total number of H2-D$^b$ gp$_{33–41}$–specific splenocytes in WT versus *Runx2$^{fl/fl}$* mice at days 9, 14, and 28 postinfection. (**C**) KLRG1 versus CD127 staining of WT and *Runx2$^{fl/fl}$* CD8$\alpha^+$ CD44$^{hi}$ and H2-D$^b$ gp$_{33–41}$ tetramer$^+$ splenocytes at days 9, 14, and 28 postinfection. (**D** and **E**) Total number of H2-D$^b$ gp$_{33–41}$–specific TECs (D) and MPCs (E) in WT versus *Runx2$^{fl/fl}$* mice at days 9, 14, and 28 postinfection. (**F**) Cells were restimulated with gp$_{33–41}$ peptide for 4 h in vitro. Total number of H2-D$^b$ gp$_{33–41}$–specific IFN-$\gamma^+$, TNF-$\alpha^+$, and IL-2$^+$ splenocytes (triple producers) in WT versus *Runx2$^{fl/fl}$* CD8$\alpha^+$ and CD44$^{hi}$ cells at days 9, 14, and 28 after LCMV–Armstrong infection. (**G**) WT C57/BL6 mice were infected with LCMV–Armstrong and analyzed on day 9 postinfection for Runx2 expression levels in CD8$\alpha^+$, CD44$^{hi}$ H2-D$^b$ gp$_{33–41}$, gp$_{276–286}$, and np$_{396–404}$–specific MPCs versus TECs. (**H**) Normalized mean fluorescence intensity (MFI) of Eomes, TCF-1, and T-bet in H2-D$^b$ gp$_{33–41}$ tetramer-specific WT versus *Runx2$^{fl/fl}$* splenocytes were analyzed at days 9,14, and 28 after LCMV–Armstrong infection by staining for Eomes, TCF-1, or T-bet. Data show normalized MFI for transcription factor staining in gated CD8$\alpha^+$ and CD44$^{hi}$ H2-D$^b$ gp$_{33–41}$ tetramer$^+$ cells. Samples were normalized to average MFI value for each protein in the WT samples in each experiment. Data are from three independent experiments with a total of 9–12 mice per group per time point. Data from (F) are from two independent experiments with a total of 12 mice. *$p \leq 0.05$, **$p \leq 0.01$, ***$p \leq 0.001$, ****$p \leq 0.0001$. ns, $p > 0.05$.

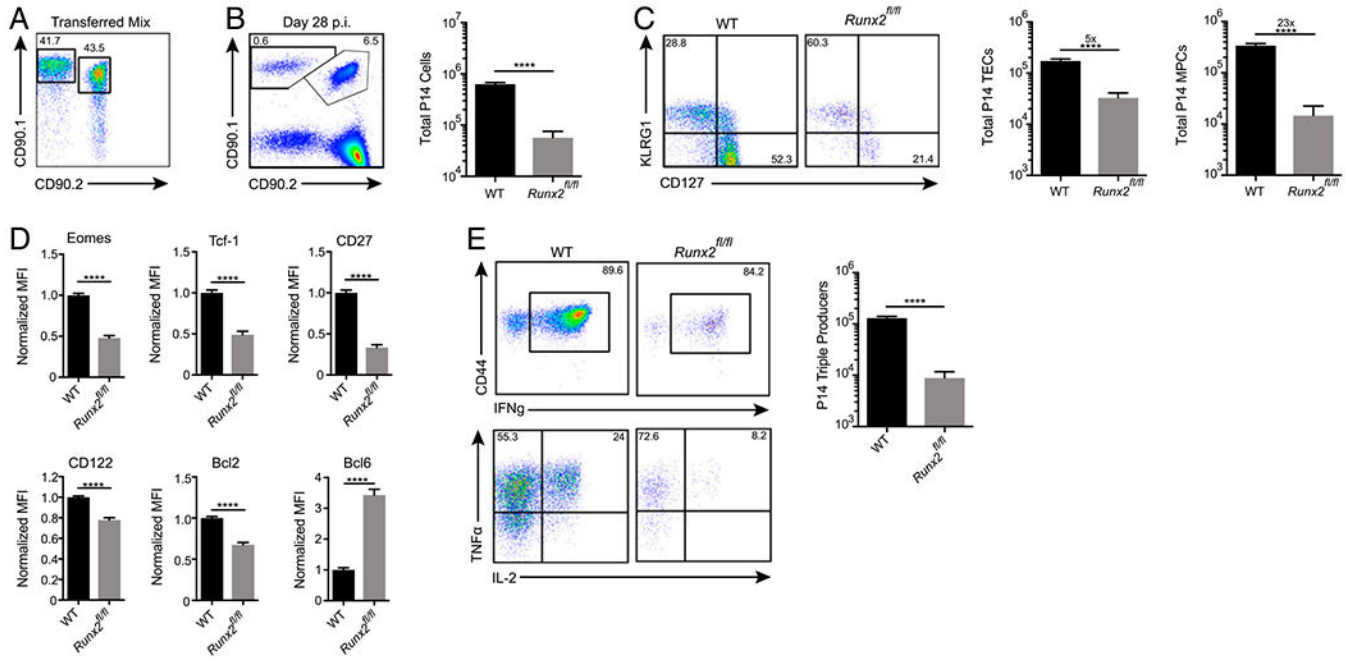


**FIGURE 2. Loss of pathogen-specific T cell memory is due to the absence of Runx2 in CD8$^+$ T cells.**

WT P14 (CD90.1$^+$/CD90.2$^+$) and *Runx2$^{fl/fl}$* P14 cells (CD90.1$^+$) were mixed 1:1 and transferred into WT (CD90.2$^+$) recipients. (**A**) Mixture of donor T cells prior to transfer. (**B**) One day after transfer, recipient mice were infected with LCMV–Armstrong, and splenocytes were analyzed on day 28 postinfection. WT P14 (CD90.1$^+$/CD90.2$^+$) and *Runx2$^{fl/fl}$* P14 (CD90.1$^+$) cells are shown (left), and the total numbers of WT P14 and *Runx2$^{fl/fl}$* P14 splenocytes at day 28 postinfection were compiled (right). (**C**) Cells were stained for KLRG1 and CD127, and donor populations were gated (left); total numbers of WT P14 and *Runx2$^{fl/fl}$* P14 TECs (middle) and MPCs (right) in host mice at day 28 postinfection are shown. (**D**) Normalized expression of Eomes, TCF-1, CD27, CD122, Bcl2, and Bcl6 at day 28 postinfection. Mean fluorescence intensity (MFI) values are normalized to the average of WT P14 cells analyzed in each sample. (**E**) Cells were restimulated with $gp_{33–41}$ peptide for 4 h in vitro and stained for intracellular IFN-$\gamma$, TNF-$\alpha$, and IL-2 as shown (left). Total numbers of H2-D$^b$ $gp_{33–41}$–specific IFN-$\gamma^+$, TNF-$\alpha^+$, and IL-2$^+$ splenocytes (triple producers) in WT versus *Runx2$^{fl/fl}$* P14 cells at day 28 after LCMV–Armstrong infection are shown (right). Data are from two independent experiments with a total of nine mice. ****$p \leq 0.0001$.

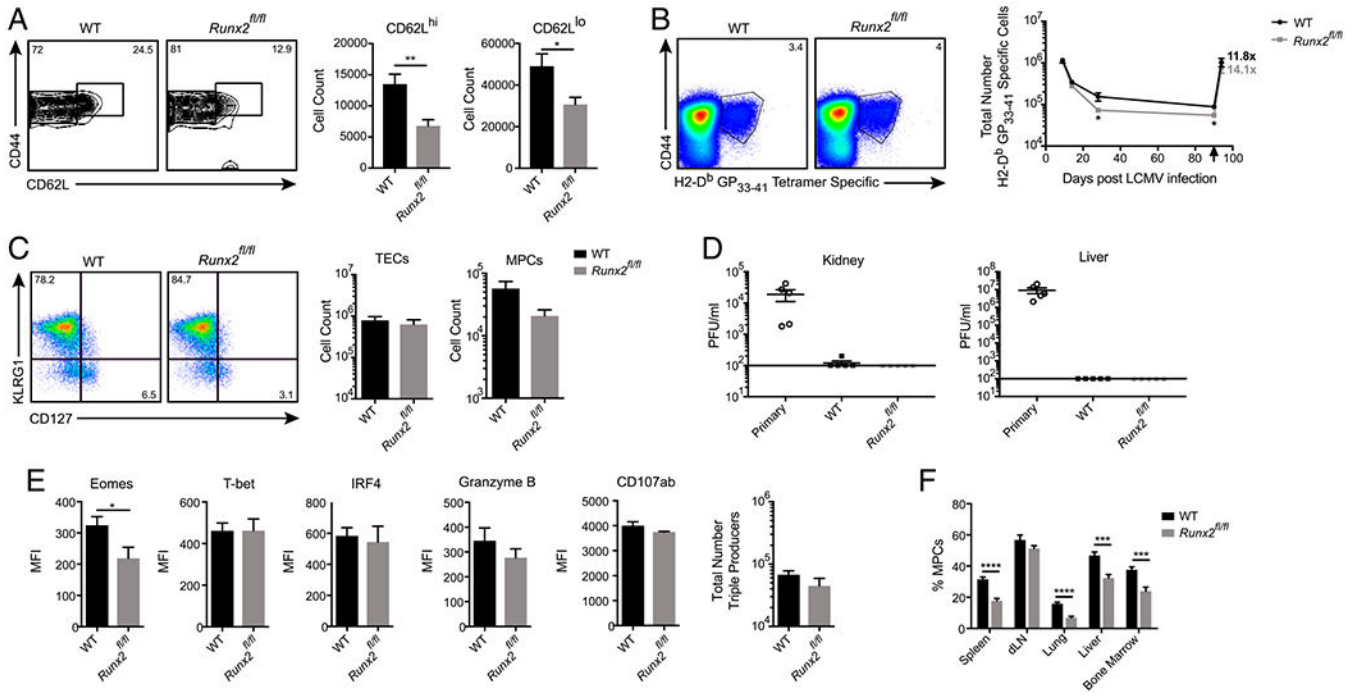


**FIGURE 3. Runx2 deficiency in T cells does not impair the recall response to LCMV.**

WT and *Runx2*$^{fl/fl}$ mice were infected with LCMV–Armstrong and were rechallenged on day 90 postinfection with a high dose of LCMV–clone 13. (**A**) Splenocytes were analyzed on day 90 prior to secondary challenge for CD44$^{hi}$ CD62L$^{hi}$ staining (gated H2-D$^{b}$ gp$_{33–41}$ tetramer$^{+}$ CD8$^{+}$ cells) (left) as well as total numbers of CD62L$^{hi}$ cells (center) and CD62L$^{lo}$ cells (right). (**B**) H2-D$^{b}$ gp$_{33–41}$ tetramer$^{+}$ CD8$^{+}$ CD44$^{hi}$ staining is shown on day 4 after rechallenge (left). Time course of virus-specific cells including day 4 after LCMV–clone 13 rechallenge is shown (right). (**C**) H2-D$^{b}$ gp$_{33–41}$–specific CD8$^{+}$ cells were stained for KLRG1 and CD127 at day 4 after LCMV–clone 13 rechallenge (left), and total cell numbers of H2-D$^{b}$ gp$_{33–41}$–specific TECs (center) and MPCs (right) were quantified. (**D**) Plaque assay of LCMV titers in kidney and liver on day 4 after LCMV–clone 13 rechallenge. (**E**) Mean fluorescence intensity (MFI) of Eomes, T-bet, IRF4, granzyme B, CD107a+b, and total number of triple producers on day 4 after LCMV–clone 13 rechallenge. Intracellular cytokine staining was performed after a 4-h gp$_{33–41}$ peptide stimulation in vitro. (**F**) Spleen, lymph node, lung, liver, and bone marrow lymphocytes were isolated on day 14 after primary infection with LCMV–Armstrong. Frequencies of H2-D$^{b}$ gp$_{33–41}$–specific MPCs in tissues from infected WT versus *Runx2*$^{fl/fl}$ mice are shown. Data from day 90 postinfection are from three independent experiments with a total of 12 mice per group. Data from LCMV–clone 13 rechallenge are from two independent experiments with a total of five mice per group. Data in (F) are from three independent experiments with a total of 9–10 mice per group. $*p \leq 0.05$, $**p \leq 0.01$, $***p \leq 0.001$, $****p \leq 0.0001$.

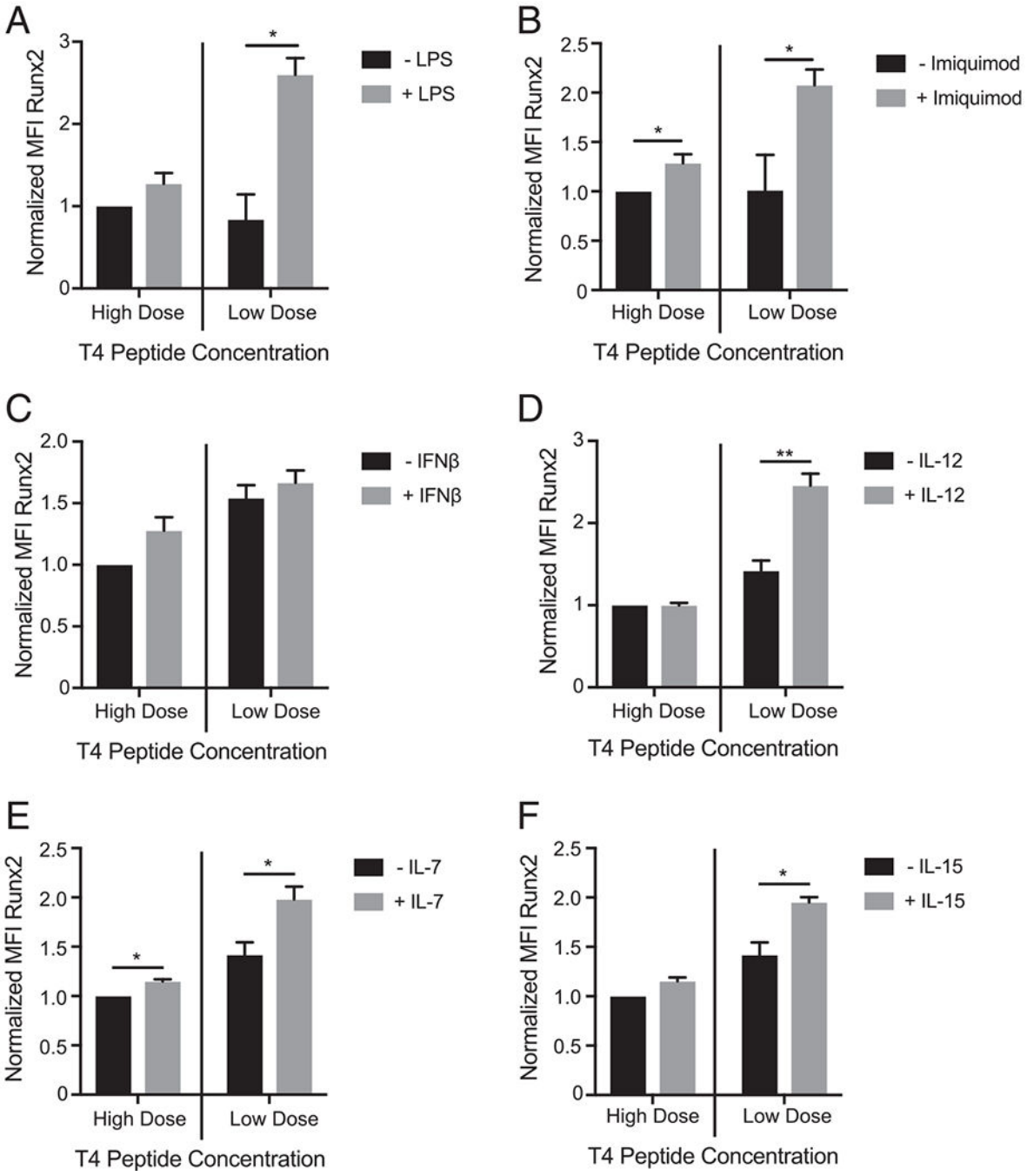


**FIGURE 4. TLR and cytokine signaling enhance Runx2 expression in vitro.**

(**A**–**F**) OT-I TCR transgenic splenocytes were isolated and cultured in vitro with high (100 nM) or low [(A and B) 0.4 nM, (C–F) 0.8 nM] doses of T4 peptide in the presence or absence of (A) LPS, (B) imiquimod, (C) IFN-β, (D) IL-12, (E) IL-7, and (F) IL-15. Cultures also contained 20 ng rIL-2 (A and B) or supernatants from IL-2 producer cells (C–F). Samples were stained for Runx2 72 h poststimulation. Graphs show mean fluorescence intensity (MFI) of Runx2 staining normalized to signal in OT-I cells stimulated with high-

dose T4 peptide in the absence of cytokine or TLR agonist. Data are representative of three to five experiments. $*p \leq 0.05$, $**p \leq 0.01$.

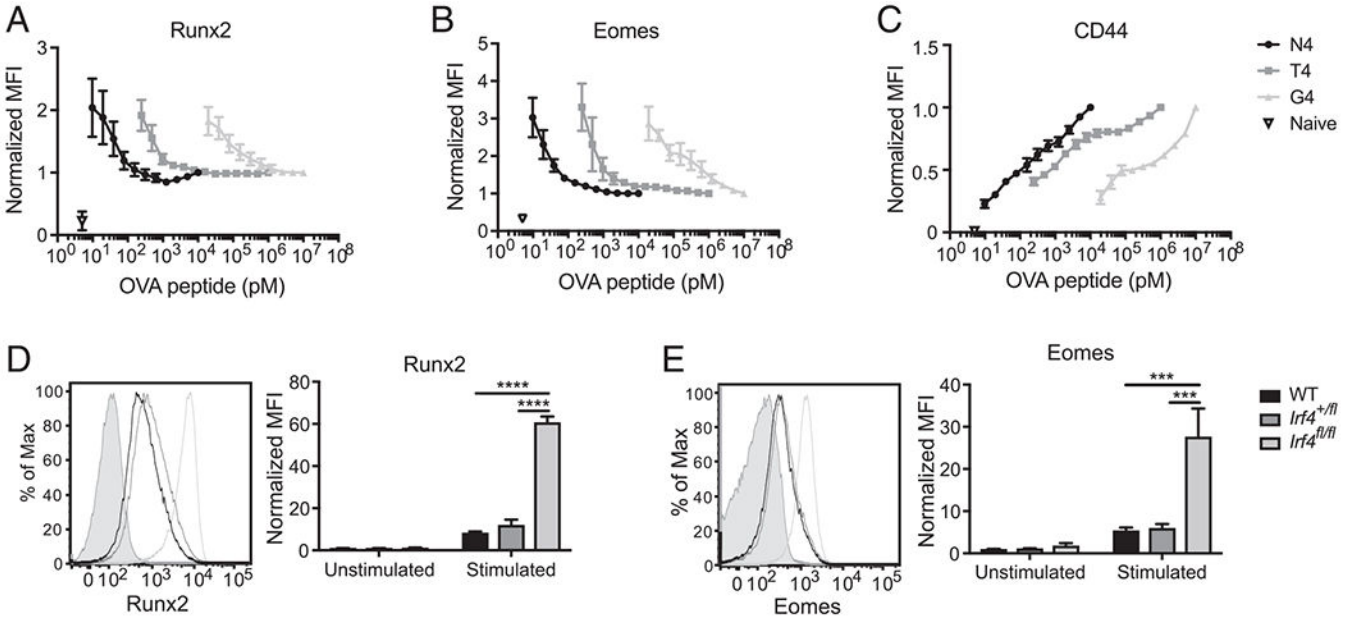


**FIGURE 5. Runx2 expression inversely correlates with TCR signal strength and Irf4 expression levels.**

(**A**–**C**) OT-I TCR transgenic splenocytes were isolated and cultured in vitro with various doses of N4, T4, or G4 peptide in the presence of supernatants from IL-2-secreting cells. After 72 h, OT-I cells were stained for (A) Runx2, (B) Eomes, and (C) CD44. Graphs show mean fluorescence intensity (MFI) of Runx2, Eomes, or CD44 staining normalized to signal in OT-I cells stimulated with 10 nM N4 peptide. (**D** and **E**) $CD8^+$ T cells were isolated from splenocytes of WT, $Irf4^{+/fl}$, or $Irf4^{fl/fl}$ mice and plated with $\alpha$CD3/28 plus IL-2 supernatants. Cells were harvested 72 h after stimulation and stained for Runx2 (D) or Eomes (E). Filled histograms show staining in naive WT OT-I cells. Graphs at right show compilations of data normalized to WT unstimulated control. Data are representative of three to five experiments. $***p \leq 0.001$, $****p \leq 0.0001$.